Concentration and Size Dependence of Dielectric Strength and Dielectric Relaxation of Polymers in Solutions of a Θ Solvent via Molecular Dynamics Simulations

Yiannis N. Kaznessis, Davide A. Hill, and Edward J. Maginn*

Department of Chemical Engineering, University of Notre Dame, Notre Dame, Indiana 46556

Received August 21, 1998; Revised Manuscript Received November 10, 1998

ABSTRACT: We consider the dielectric strength and dielectric relaxation of dilute and semidilute solutions of polymers in a Θ solvent. A molecular dynamics technique is employed and the simulation results are contrasted with dielectric spectroscopy measurements, providing an insight into the molecular factors that affect the experimental behavior. The relation between the dielectric strength and the end-to-end distance of the chains, used in experiments to determine polymer dimensions, is established via equilibrium and nonequilibrium simulations. The dielectric loss spectra are computed from the end-to-end vector autocorrelation function of the simulated systems. At infinite dilution the simulation spectra conform well with the Rouse model prediction. The spectra broaden with increasing concentration, and a normal-mode analysis suggests that the overlapping of the chains leads to a broader distribution of relaxation times. Finally, normal mode relaxation times are found to be exponential in density.

I. Introduction

We simulate polar flexible macromolecules in a Θ solvent in an attempt to interpret and elucidate experimental dielectric spectroscopy results at the molecular level. The static and dynamic properties of macromolecules in solutions of Θ solvents have been the subject of extensive theoretical[1−5] and experimental[6,7] studies. The widespread interest stems from the fact that at the Θ point the second virial coefficient is zero and binary interactions vanish. As a result, polymers assume unperturbed conformations. The screening of excluded volume interactions by the Θ solvent greatly simplifies the theoretical treatment of the conformations and the motions of polymers. The models of Rouse[8] and Zimm[9] describe the behavior of macromolecules at the Θ point at the limits of absent and dominant hydrodynamic interactions, respectively. The success of the Zimm model in predicting the properties of polymers at the Θ point at high dilution is well documented.[2] When the concentration is increased, hydrodynamic interactions are screened out and the Rouse model takes over the description of macromolecular behavior at the limit of nonentangled concentrated solutions and melts.

It is in the intermediate concentrations, from dilute to concentrated solutions, that a comprehensive theoretical treatment of the dynamic behavior is lacking.[2] Calculation of the static properties does not present any considerable difficulties. Scaling and mean field theories have elucidated the dependences of polymer size on concentration and solvent quality.[2,3] On the other hand, theoretical descriptions of dynamical behavior typically resort to the use of phenomenological models, the complexity of which increases dramatically when considering many monomers and intermediate concentrations. Solving analytically the Langevin or the Smoluchowski equations that describe the motion of polymers becomes an insurmountable task even for chains with just a few beads at low concentrations. Consequently, theoretical attempts to provide a quantitative description of the dynamics of macromolecules in solutions are faced with significant difficulties.[2,4]

Experimentally, dielectric spectroscopy of polymeric materials has greatly assisted the fundamental understanding of macromolecular behavior.[10−14] The orientational motion of polar polymers under the influence of external electric fields, known as dielectric relaxation, provides information on the macromolecular dynamic behavior. Of importance for the correct interpretation of experimental results is the knowledge of the relative directions of the monomeric dipole and the chain contour. Type-A polar polymers, following Stockmayer's classification,[15] have their dipoles aligned in the direction parallel to the chain backbone. Consequently, the cumulative chain dipole moment **M** is proportional to the end-to-end vector **R**

$$\mathbf{M} = \mu' \mathbf{R} \tag{1}$$

where μ' is the dipole moment per unit contour of the chain.

Thus, dielectric relaxation measurements can reveal information on the global rotational motion of the chains. More specifically, the experimentally calculated complex dielectric permittivity ϵ^* is related to the normalized decay function $a(t)$ through

$$\frac{\epsilon^*(\omega) - \epsilon_\infty}{\epsilon_s - \epsilon_\infty} = \int_0^\infty \left[-\frac{\mathrm{d}a(t)}{\mathrm{d}t} \right] \exp(-i\omega t)\, \mathrm{d}t \tag{2}$$

with $\epsilon^* = \epsilon' - i\epsilon''$, where ϵ' is the real dielectric permittivity and ϵ'' is the dielectric loss. ϵ_s and ϵ_∞ are the low and high-frequency limits of the static permittivity. The normalized decay function $a(t)$ determines the linear response of a polar system when a small external electric field, imposed at $t = -\infty$, is suddenly removed at $t = 0$ and the dipoles reorient themselves to an equilibrium distribution.

According to the fluctuation−dissipation theorem,[17] $a(t)$ is congruent to the time correlation function of the dipole moment of the chains, **M**. Consequently, for type-A polymers, $a(t)$ is congruent to the total time correlation function $\phi(t)$ of the end-to-end vector **R**. $\phi(t)$ is given by

10.1021/ma981320u CCC: $18.00
Published on Web 01/30/1999

$$\phi(t) = \frac{\langle \sum_{i=1}^{M_c} \mathbf{R}_i(0) \cdot \sum_{k=1}^{M_c} \mathbf{R}_k(t) \rangle}{\langle \sum_{i=1}^{M_c} \mathbf{R}_i(0) \cdot \sum_{k=1}^{M_c} \mathbf{R}_k(0) \rangle} \quad (3)$$

where M_c is the number of chains in the system.

It has been argued extensively that the cross-correlation terms, $\mathbf{R}_i(0) \cdot \mathbf{R}_k(t)$, $k \neq i$, are negligible for flexible chains in homogeneous environments.[13] This contention was clearly established by MD simulations of type-A polar macromolecules in good solvents.[16] Consequently, the total time correlation function is reduced to the autocorrelation function

$$\phi(t) = \frac{\langle \mathbf{R}(0) \cdot \mathbf{R}(t) \rangle}{\langle \mathbf{R}(0) \cdot \mathbf{R}(0) \rangle} \quad (4)$$

where the brackets indicate ensemble averages. Equations 2 and 4 thus give a prescription for calculating dielectric spectra from equilibrium simulations.

Dielectric spectroscopy can also assist in the determination of the molecular structure through a connection of the dielectric constant and molecular dipole moments. Specifically, the static properties of type-A chains can be determined from the relation between the dielectric strength $\Delta\epsilon$ and the mean squared end-to-end distance $\langle R_{eq}^2 \rangle$ at equilibrium as calculated by means of statistical mechanics arguments[13]

$$\Delta\epsilon = \frac{4\pi N_A \mu'^2 \langle R_{eq}^2 \rangle CF}{3 k_B T M_w} \quad (5)$$

where N_A is the Avogadro number, μ' is the dipole moment per unit contour length of the chain, T is the temperature, k_B is the Boltzmann factor, M_w is the molecular weight, C is the concentration, and F is the ratio of the effective-local field to the applied field (as discussed in ref 13, $F \simeq 1$ for the case of type-A polymer solutions).

Adachi and Kotaka have investigated extensively type-A chains in Θ solvents using dielectric spectroscopy techniques.[13,18,19] Specifically, they examined the dielectric relaxation of *cis*-polyisoprene (PI), a type-A polymer, in dilute, semidilute and concentrated solutions of dioxane, a Θ solvent at 308 K. They examined the concentration and size dependence of the dielectric relaxation time and the shape of the dielectric loss spectra. For high dilutions the spectra have shapes consistent with the Rouse/Zimm theory. For semidilute and concentrated solutions the spectra broaden. This behavior cannot be explained in terms of existing theories and it was attributed to overlapping of the chains and entanglement effects. Nevertheless, it is not entirely clear how these factors affect the distribution of relaxation times. Adachi and Kotaka also calculated the end-to-end distance $\langle R^2 \rangle$ from the dielectric strength $\Delta\epsilon$ and determined the dependence of the macromolecular dimensions on the concentration and the chain length.

In this paper, we simulate flexible type-A polymers in dilute and semidilute solutions of a Θ solvent, using a molecular dynamics technique. Simulations are an established method for the study of macromolecular systems.[20−22] They are widely accepted as a means of providing insight into experimentally observed phenomena and validating existing theories. The main objective of our work is to complement the dielectric spectroscopy measurements by explaining the experimentally observed phenomena at the molecular level. We employ a commonly used bead−spring model[16,23,24] for the chains and adjust the simulation temperature so that the polymers attain their unperturbed conformations at infinite dilution.

Previous numerical investigations of the behavior of polymers at the Θ point include Brownian dynamics simulations[25−30] and Monte Carlo techniques,[31−34] an excellent review of which can be found in ref 20. Monte Carlo is an efficient technique for computing the static properties of polymers. However, the artificial nature of the moves used in a Monte Carlo scheme does not allow for direct quantitative comparison of dynamic properties with experimental results. Brownian dynamics (BD) simulations are based on the numerical solution of the Langevin differential equation or its equivalent Smoluchowski diffusion equation. They have the advantage of being able to cope with hydrodynamic effects,[25] but the intensive computational requirements of the calculations have allowed for only moderate system sizes to be studied.

We examine chains with up to $N = 200$ beads at concentrations ranging from infinite dilution to the semidilute regime. The main assumption of our model is the neglect of hydrodynamic interactions (HI). This neglect leads to severe quantitative deviations from the experimental results at low concentrations. It is expected, however, that the bead−spring model will capture more accurately the dynamic behavior of macromolecules with increasing concentration, since HI are effectively screened out for concentrated systems.[2] Kremer and Grest established this for dense polymer systems, simulating macromolecules with this model.[23] Moreover, in ref 16, we simulated flexible type-A polar polymers in dilute and semidilute solutions of a good solvent neglecting HI and compared our results with experimental dielectric spectroscopy measurements. We found that at relatively low densities the simulations conform remarkably well with the experiment. When the simulation model parameters were mapped to properties of polyisoprene, the results were in near perfect agreement with the mapping determined by Kremer and Grest, who compared their simulations of polymer melts with diffusion and viscoelasticity experiments.[23] By inference, we concluded that hydrodynamic interactions are screened out at relatively low concentrations. It would be very interesting to determine the concentration range over which HI are important using molecular dynamics simulations. However, this would require the inclusion of explicit solvent molecules, rendering the computations exceedingly demanding for present computers.

In addition, the bead−spring model is in excellent qualitative agreement with the dynamic behavior observed by Adachi and Kotaka[13,18,19] throughout the whole concentration range. Indeed, the Rouse and Zimm models predict the same form for the autocorrelation function of the end-to-end vector, hence same dielectric spectra,[8,9] implying that HI do not affect significantly $\phi(t)$ or $\epsilon^*(\omega)$.

We use both equilibrium and nonequilibrium simulations to investigate the relationship of $\Delta\epsilon$ and $\langle R^2 \rangle$ and the dependence of the chain dimensions on the concentration and the length of the chain. The dielectric spectra are calculated from the autocorrelation function of the end-to-end vector. The normal mode relaxation times are determined and the shape of the dielectric loss

curve is studied for different densities and chain sizes.

The rest of the paper is organized as follows. In section II the simulation methodology is described. In section III the simulation results are presented. The connection between the dielectric strength and the equilibrium chain dimensions is established. Then, the equilibrium static properties of the chains are investigated. Finally, dynamic properties, such as correlation functions, dielectric spectra and normal mode relaxation times are studied. In section IV the conclusions of our work are summarized.

II. Simulations Model and Technique

The employed bead−spring model has been used extensively to simulate polymers in good solvents at infinite dilution,[24] dilute and semidilute solutions,[16] and melts.[23] It has also been used in simulations of grafted polymer brushes in solvents of varying quality,[35] including the Θ point. Since details of the simulation technique can be found in the references above, we shall only present the most important features of the model.

Each of the monomers is coupled with a heat bath, which is the source of random forces $\mathbf{F}_i$ that follow a Gaussian white-noise pattern

$$\langle F_i(t)F_j(t)\rangle = 2\xi k_B T m \delta_{ij}\delta\,(t - t') \tag{6}$$

with $\langle F_i\rangle = 0$. In eq 6, m is the mass of the beads, k_B is the Boltzmann factor and T is the simulation temperature. ξ is the coefficient of the friction force on each bead that couples the beads to the heat bath

$$\mathbf{F}_{ri}(t) = -m\xi\frac{d\mathbf{r}_i}{dt} \tag{7}$$

where $d\mathbf{r}_i/dt$ is the velocity of the ith bead.

A truncated Lennard−Jones potential

$$U_{LJ}(r_{ij}) = \begin{cases} 4\epsilon\left[\left(\frac{\sigma}{r_{ij}}\right)^{12} - \left(\frac{\sigma}{r_{ij}}\right)^{6}\right], & r \le r_c \\ 0 & r > r_c \end{cases} \tag{8}$$

is employed for the bead−bead interactions, where $r_{ij} = |r_{ij}| = |r_i - r_j|$, σ is the bead size, ϵ is the Lennard−Jones interaction parameter and the cutoff radius $r_c = 2.5\sigma$.

Any two consecutive beads along a chain interact through a frictionless FENE spring potential

$$U_{bnd}(r_{ij}) = \begin{cases} -0.5kR_o^2\ln[1 - (r_{ij}/R_o)^2], & r \le R_o \\ \infty & r > R_o \end{cases} \tag{9}$$

The parameters $k = 30\epsilon/\sigma^2$ and $R_o = 1.5\sigma$ are the same as in ref 23.

We consider our chains as being type-A polar macromolecules with a global permanent dipole μ. The dipoles can be replaced by a pair of charges q and $-q$ located at the center of mass of the end beads. Consequently, the dipole vector for the jth chain is $\boldsymbol{\mu}_j = q(\mathbf{r}_N - \mathbf{r}_1)$. We neglect dipole−dipole interactions because, for the magnitudes of dipoles studied, these interactions have a negligible effect on the static and dynamic properties of the chains.[36] Consequently, Coulombic interactions between different charges are not taken into account. However, when external electric fields are imposed on the system the end beads feel an additional force

$$\mathbf{F}_{Ei} = q_i\mathbf{E} \tag{10}$$

The equation of motion for each bead i is

$$m\frac{d^2\mathbf{r}_i}{dt^2} - \nabla(U_{LJ} + U_{bnd}) - m\xi\frac{d\mathbf{r}_i}{dt} + \mathbf{F}_i + \mathbf{F}_{Ei} \tag{11}$$

Equation 11 is solved for all the beads using a fifth-order predictor corrector scheme, with a time step $\Delta t = 0.008\,\tau$, where $\tau = \sigma(m/\epsilon)^{1/2}$ is the characteristic time of the system. Reduced units are used so that $\epsilon = \sigma = m = 1.0$. The friction coefficient is $\xi = 0.5\tau^{-1}$, a value commonly used.[16,23−25]

Grest and Murat[35] estimated the Θ temperature by simulating chains in homogeneous solutions at infinite dilution with the same model we have adopted. At the Θ point chains assume unperturbed conformations[2] and their average squared radius of gyration scales with the number of beads as $\langle R_G^2\rangle \propto N$. By simulating systems with different numbers of beads at different temperatures they found that $T_\Theta = (3.0 \pm 0.1)\epsilon/k_B$. Although their chains were nonpolar, the Θ temperature is expected to be the same for the present study, since electrostatic interactions have been neglected. Consequently, here we adopt $T = 3.0\epsilon/k_B$.

For the nonequilibrium simulations the dipole moment per unit chain contour is $\mu' = \mu_{nr}/(4\pi\epsilon_o\epsilon_{solv}\sigma\epsilon)^{1/2} = 1.0$, where μ_{nr} is the nonreduced dipole per unit chain contour, ϵ_o is the vacuum permittivity, and ϵ_{solv} is the permittivity of the solvent. The reduced applied electric fields range from $E = 0.05$ to $E = 0.35$, with $E = E_{nr}/(4\pi\epsilon_o\epsilon_{solv}\sigma^3\epsilon^{-1})^{-1/2}$, where E_{nr} is the nonreduced electric field. These field magnitudes produce linear system responses. More details can be found in refs 16 and 36.

Initial configurations are obtained with a self-avoiding random walk scheme, and the systems are equilibrated for times longer than the longest configurational relaxation time. Systems with M_c chains are studied, each with $N = 30$−200 beads at reduced densities $\rho = NM_c/L^3 = 0.0$, 0.01, 0.03, 0.10, 0.20, 0.30, and 0.40. L is the simulation box length in units of σ. Infinite dilution systems are studied by turning off the intermolecular potential.

III. Results

III-1. Dielectric Strength and Polymer Dimensions. It is of interest to study the dimensions of type-A polar polymers under the influence of external electric fields to assess the validity of eq 5. Systems of chains with $N = 30$ beads at different densities ρ are brought to a steady state under the influence of homogeneous, local electric fields E. The ensemble average of the chain dipole moments in the direction of the field $\langle\mu_{field}\rangle$ is calculated at the steady state as a function of E. The dimensions of the polymers are also calculated both at equilibrium and at steady states as a function of E. Specifically, the ensemble average squared end-to-end distance $\langle R^2\rangle$ and the ensemble average squared radius of gyration are calculated as

$$\langle R^2\rangle = \langle(\mathbf{r}_1 - \mathbf{r}_N)^2\rangle \tag{12}$$

and

$$\langle R_G^2\rangle = \frac{1}{N}\left\langle\sum_{i=1}^{N}(\mathbf{r}_i - \mathbf{r}_{cm})^2\right\rangle \tag{13}$$

Table 1. Equilibrium Squared End-To-End Distance $\langle R^2 \rangle$ and Nonequilibrium Chain Polarization $\langle \mu_{field} \rangle$ for Systems of Chains with Size N, at Densities ρ, Under the Influence of Electric Fields E

N	ρ	E	$\langle R^2 \rangle$	$\langle R_G^2 \rangle$	$\langle \mu_{field} \rangle$
30	0.03	0.00	44.83	7.69	
30	0.03	0.10	46.25	7.72	0.483
30	0.03	0.17	47.01	7.74	0.814
30	0.03	0.25	47.52	7.78	1.259
30	0.03	0.30	47.96	7.81	1.502
30	0.03	0.35	49.27	8.00	1.775
30	0.10	0.00	47.90	7.83	
30	0.10	0.10	47.99	7.84	0.508
30	0.10	0.17	48.35	7.88	0.865
30	0.10	0.25	48.87	7.90	1.239
30	0.10	0.30	49.22	7.98	1.582
30	0.10	0.35	50.46	8.02	1.804
30	0.30	0.00	50.62	8.02	
30	0.30	0.10	50.37	7.99	0.557
30	0.30	0.17	50.64	8.03	0.961
30	0.30	0.25	50.87	8.11	1.444
30	0.30	0.30	51.03	8.18	1.676
30	0.30	0.35	51.61	8.19	1.917

respectively, where r_{cm} is the chain center of mass. The results of the simulations are shown in Table 1. The electric fields employed range between $E = 0.10$ and 0.30 and produce responses in the linear regime.[16] The size of the polymers increases appreciably, when strong fields are applied on the dilute systems. For denser systems the expansion is less pronounced, indicating the prominent role of the intermolecular interactions over the electrostatic ones. For all densities, there is a measurable dipole moment buildup in the direction of the field. The fact that $\langle \mu_{field} \rangle$ increases more with increasing E than the chain dimensions at $\rho = 0.3$ suggests that only the ends orient themselves in the direction of the field. For less dense systems larger parts of the chains are oriented in the direction of the field, leading to more expanded dimensions.

The dielectric strength for a system with n_p dipoles per unit volume is

$$\Delta\epsilon = \frac{4\pi n_p \langle \mu_{field} \rangle}{E} \tag{14}$$

and the mean end-to-end distance at $E = 0$ is from eq 5

$$\langle R_{eq}^2 \rangle = \frac{3k_B T \langle \mu_{field} \rangle}{E\mu'^2 F} \tag{15}$$

In the simulations the electric field applied is the local, effective field, i.e., $F = 1$. In Figure 1 we plot the right-hand side of eq 15 as a function of the electric field magnitude E for two densities $\rho = 0.03$ and $\rho = 0.30$. Also shown in Figure 1 are the mean squared end-to-end distances $\langle R_{eq}^2 \rangle$ of the two systems for $E = 0$. It is seen that within the statistical errors of the equilibrium and nonequilibrium simulations, eq 15 and hence eq 5 are valid for the simulated systems and conditions. More susceptible to error are the nonequilibrium calculations of the less dense systems, since the signal-to-noise ratio has low values.

III-2. Equilibrium Chain Dimensions. Equilibrium simulations are employed to calculate the static properties of the polymers and investigate their concentration and chain size dependence. The calculated end-to-end distance and the radius of gyration are shown in Table 2 for a number of systems of chains with N beads at densities ρ.

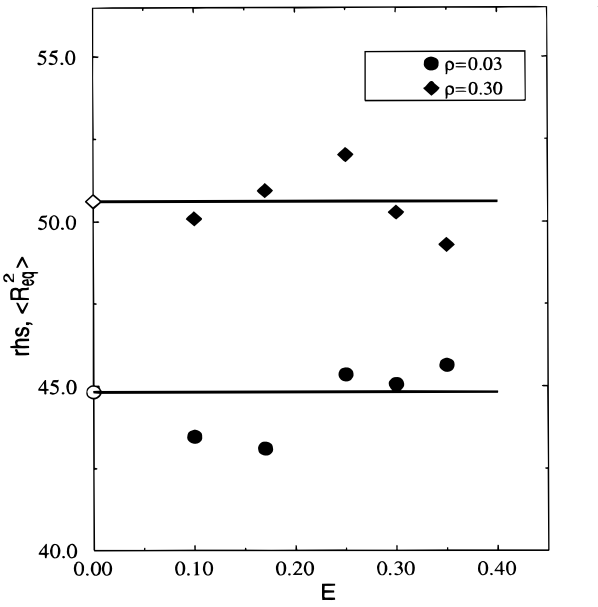

Figure 1. Right-hand side of eq 15, $rhs = (3k_B T\langle \mu_{field} \rangle)/(E\mu'^2 F)$, as a function of the electric field E, for systems with $N = 30$ at densities $\rho = 0.03$ and 0.30. The open symbols give the equilibrium mean squared end-to-end distances $\langle R_{eq}^2 \rangle$ of the two systems. Straight lines are drawn to guide the eye.

Table 2. Static Properties and Normal Mode Relaxation Times for Systems of Chains with size N, at Densities ρ Where the Systems were Simulated for Times T/τ

N	ρ	T/τ	$\langle R^2 \rangle$	$\langle R_G^2 \rangle$	τ
50	0.00	6400	78.7	13.29	29.1
50	0.01	6400	78.8	13.30	31.9
50	0.03	6400	79.9	13.47	32.7
50	0.10	6400	82.4	13.76	52.1
50	0.20	8000	84.4	13.99	68.9
50	0.30	8000	84.2	13.97	92.7
50	0.40	8000	81.3	13.72	127.3
75	0.00	8000	118.0	20.04	57.2
100	0.00	8000	159.2	27.08	110
100	0.01	14400	160.1	27.22	115
100	0.03	14400	162.5	27.49	130
100	0.10	14400	172.2	28.82	205
100	0.20	14400	173.6	29.21	280
100	0.30	22400	179.4	30.19	395
100	0.40	22400	175.3	29.98	560
150	0.00	14400	236.2	40.61	235
150	0.01	14400	238.9	40.76	255
150	0.03	14400	240.4	41.47	295
150	0.10	22400	262.7	43.95	495
150	0.20	22400	280.7	46.66	665
150	0.30	22400	267.2	46.98	1050
150	0.40	36000	255.6	43.77	1390
200	0.00	10000	311.8	53.82	420

In Figure 2 the average squared end-to-end distance and the average squared radius of gyration are plotted vs the size of the chains for systems at infinite dilution. Power law dependences $\langle R^2 \rangle \propto N^{1.0}$ and $\langle R_G^2 \rangle \propto N^{1.0}$ are observed in accordance with the Flory theory for unperturbed chains.[1] It can also be observed that $\langle R^2 \rangle = 6.0\langle R_G^2 \rangle$, within the statistical accuracy of the simulations, as the theory indicates.[1]

Adachi and Kotaka[18] determined $\langle R^2 \rangle$ for PI at high dilution in dioxane from dielectric strength measurements and from ref 18 we extracted the relation $\langle R^2 \rangle \simeq 8.31 \times 10^{-17} M_w$ cm^2, where M_w is the molecular weight. Adachi and Kotaka stressed that the results are subject to errors on the order of 20%, steming from errors entering the calculation of the PI dipole per unit contour and the dielectric strength. However, we can now

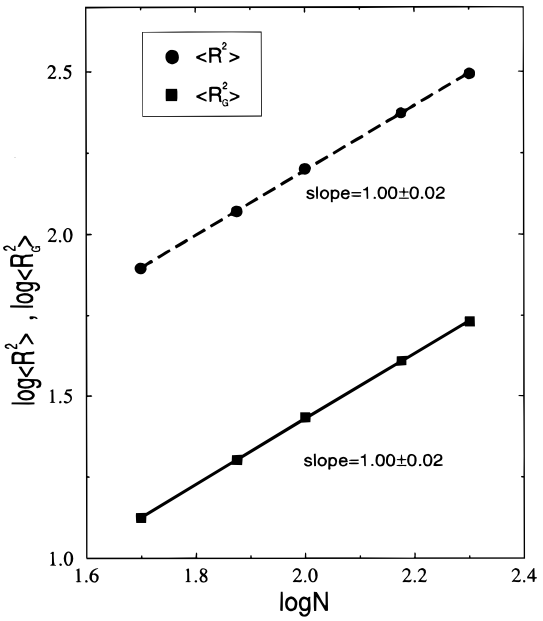

Figure 2. Mean squared end-to-end distance $\langle R^2 \rangle$ and average squared radius of gyration $\langle R_G^2 \rangle$ vs the number of beads N for systems at infinite dilution.

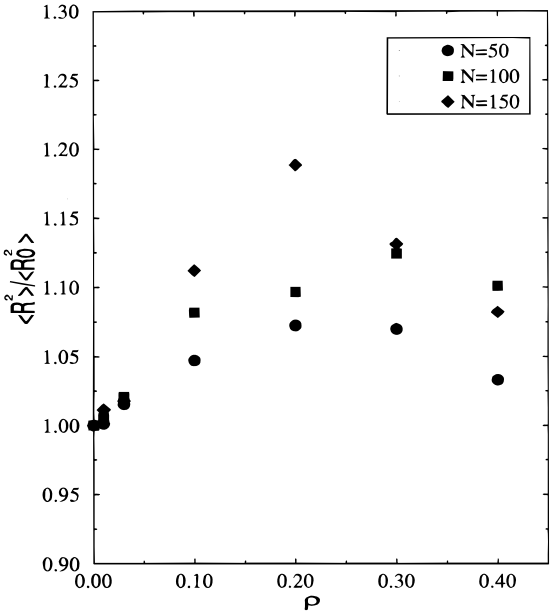

Figure 3. Ratio of the mean squared end-to-end distance over the average squared end-to-end distance at infinite dilution, $\langle R_o^2 \rangle$, vs the density ρ.

proceed to a mapping of our model parameters to PI properties. From the simulations we find an average bond length $l = 0.936\sigma$ and from $\langle R^2 \rangle = (l l_p)^2(N - 1)$ we find a persistence length $l_p \simeq 1.34$, expressed in number of monomers. The characteristic ratio C_∞ ($C_\infty = l_p^2$) for PI has been determined to be $C_\infty = 5.0$.[6] We can therefore conclude that one model bead is approximately 1.67 monomers of PI and that $1\sigma \simeq 0.75$ nm.

Increasing the concentration in a Θ solvent should result in no changes in the dimensions of the chains, according to theoretical predictions.[2] In Figure 3 the ratio of the mean squared end-to-end distance over the average squared end-to-end distance at infinite dilution, $\langle R_o^2 \rangle$, is plotted against the density. Significant deviations from the unperturbed state are observed. The chain size initially increases with increasing density. For longer chains the expansion is more pronounced. For denser systems, the end-to-end distances contract, seemingly saturating to the infinite dilution dimensions again. At first glance, this behavior might be explained by questioning the estimated Θ temperature. The chain dimension trends suggest that the chains might be slightly collapsed, i.e., the actual Θ temperature for the model is higher than the proposed $T_\theta = 3.0\epsilon/k_B$. However, the scaling of the chain dimensions with the number of the beads is the one theoretically predicted for the Θ point. This scaling is quite sensitive to temperature. We have performed simulations for infinite dilution systems at $T = 2.8\epsilon/k_B$ and $T = 3.2\epsilon/k_B$ and found considerable deviations from the $\langle R_G^2 \rangle \propto N^{1.0}$ scaling. Moreover, the same behavior was observed from other simulations that have employed a variety of different models and techniques.[31,34,37,38] This dimensions expansion at dilute solutions of Θ solvent was explained by Olaj and Pelinka in terms of pair distribution functions $g(r)$.[37] They suggest that since $g(r)$ is not unity for all the distances between the centers of mass of two chains, contrary to the theoretical assumption, there exist residual polymer−polymer interactions that lead to the observed expansion. It is not unambiguously clear, however, whether the expansion observed at moderate concentrations is an inherent characteristic of the models used or represents real polymer behavior. In dielectric spectroscopy experiments,[13] similar behavior has been observed but Adachi and Kotaka suggest that the results are subjected to experimental errors not allowing an accurate determination of chain dimension trends with concentration in a Θ solvent.

The chains begin to overlap at higher concentrations. According to scaling theories,[2,3] the crossover density ρ^* at which overlapping occurs is

$$\rho^* = \frac{3N}{4\pi \langle R_G^2 \rangle^{3/2}} \tag{16}$$

The crossover density can be viewed as the density at which intermolecular interactions become important. Using eq 16 the crossover densities for the systems considered here are $\rho^*_{50} = 0.246$, $\rho^*_{100} = 0.169$ and $\rho^*_{150} = 0.138$ for chains with $N = 50$, 100 and 150 beads, respectively.

Polymers at and around their Θ point exhibit random-walk (RW) behavior.[2] This RW behavior is illustrated clearly by calculating the single-chain static structure factor

$$S(k) = \frac{1}{N} \langle | \sum_{n=1}^{N} \exp(i\mathbf{k}\cdot\mathbf{r}_n) |^2 \rangle \tag{17}$$

where k is the wave-vector with units of inverse length. For RW systems $S(k)$ scales as $S(k) \propto k^{-2.0}$ in the range $R_G^{-1} \ll k \ll \sigma^{-1}$.[2] In Figure 4 we plot the structure factor as a function of the wave vector for chains with $N = 50$, $N = 100$ and $N = 150$ at $\rho = 0.03$. The slope of $S(k)$ is around −2 for these and all of the systems investigated.

III-3. Dielectric Relaxation and Loss Spectra. Time correlation functions of the end-to-end vector $\phi(t)$ are calculated with eq 4 and are plotted in Figure 5 for systems at infinite dilution. At long times they decay as single exponentials. At short time scales there is a distribution of relaxation times, the nature of which can be elucidated by examining the dielectric loss spectra.

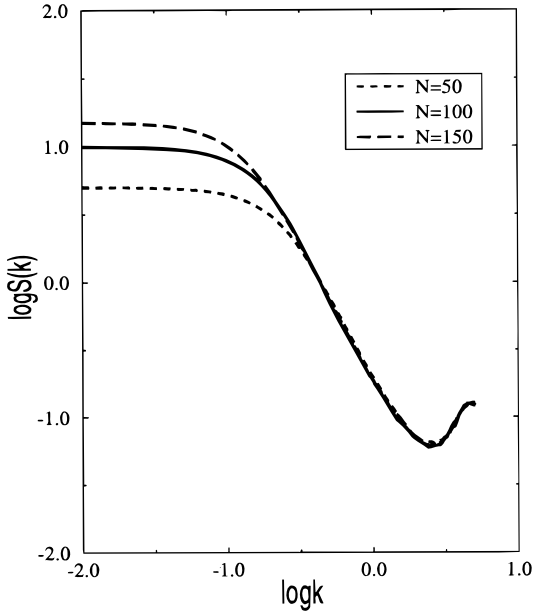

Figure 4. Single-chain structure factor $S(k)$ as a function of the wavevector k at $\rho = 0.03$.

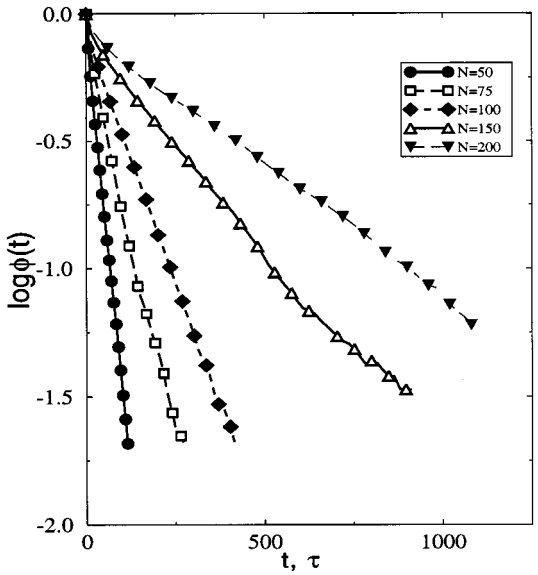

Figure 5. Logarithm of the autocorrelation function $\phi(t)$ vs time for chains with N beads at infinite dilution.

Taking the Fourier−Laplace transform of $\phi(t)$ yields the reduced dielectric loss spectra $E'' = \epsilon''/\Delta\epsilon$. In Figure 6 we plot the normalized dielectric spectra for systems at infinite dilution. It is seen that the shape of the spectra, i.e., the nature of the relaxation, is the same for all the chain sizes. The spectra shift to lower frequencies for longer chains, indicating longer relaxation times, but it is obvious that the distribution of relaxation times is independent of the chain size.

The circles in Figure 6 are the spectrum of the Rouse model[8] given by

$$E'' = \frac{8}{\pi^2}\sum_{p}\frac{\omega\tau_p}{p^2(1+\omega^2\tau_p^2)} \quad (p\text{:odd}) \qquad (18)$$

where $\tau_p = \zeta N^2 b^2/(3\pi^2 k_B T p^2)$ is the relaxation time of the pth mode, b is the average length between beads, and ζ is the friction coefficient per bead. We have shifted the theoretical curve so that its maximum coincides with

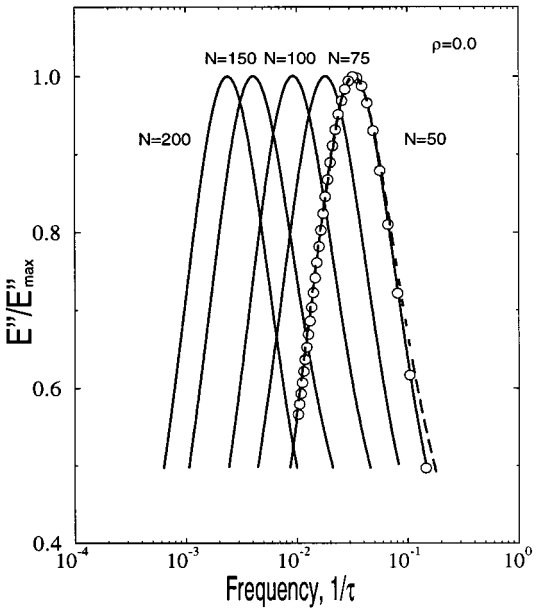

Figure 6. Normalized dielectric loss vs the frequency for systems at infinite dilution. The circles are the spectrum of the Rouse model. The dashed line is the spectrum of the Zimm model.

the maximum of the chains with $N = 50$ beads. The agreement between the simulations and the theoretical model is excellent and should be expected in view of the main assumption of our model, the neglect of hydrodynamic interactions. Hydrodynamic interactions are not treated by the Rouse model, but are accounted for in the Zimm model.[8] The spectra of the Zimm model, shown in Figure 6 (dashed line) are also given by eq 18 but with $\tau_{p\ \mathrm{Zimm}} = \pi^{3/2}\eta_s b^3 N^{3/2}/(12^{1/2} k_B T \lambda_p)$, where η_s is the solvent viscosity and λ_p is the pth eigenvalue ($\lambda_1 = 4.04$, $\lambda_3 = 24.2$, $\lambda_5 = 53.5$).[8] The shape of the Zimm model spectrum is almost identical to the Rouse spectrum, although there are some differences at the high frequency limit. Hence, it can be argued that hydrodynamic effects do not influence significantly the distribution of relaxation times of polymers. As a result, the simulations capture qualitatively the dynamic behavior of macromolecules, even at infinite dilution. The most important consequence of hydrodynamic interactions, however, is the dependence of the normal mode relaxation times on the size of the chains. The Rouse model suggests that $\tau_o \propto N^{2.0}$, whereas the Zimm model predicts that $\tau_o \propto N^{1.5}$. The simulated normal mode relaxation times are calculated as the inverse of the frequency where the maximum of the loss curve occurs. They are plotted vs the size of the chains in Figure 7. The scaling is $\tau_o \propto N^{1.94\pm0.04}$, close to the one predicted by the Rouse model. The experimental dependence conforms with the prediction of the Zimm model stressing the importance of hydrodynamic interactions. Therefore, the bead−spring model proves to be an inadequate means for quantitatively studying polymer solutions at low densities. However, it can definitely provide helpful qualitative information about the distribution of the relaxation times. In addition, the simulations should capture the experimental behavior quantitatively at higher concentrations, due to the screening of hydrodynamic interactions.

In Figure 8 the dielectric loss spectra are plotted vs the frequency for systems with $N = 50$ (a) and $N = 150$ (b) at all the densities studied. The spectra shift to lower

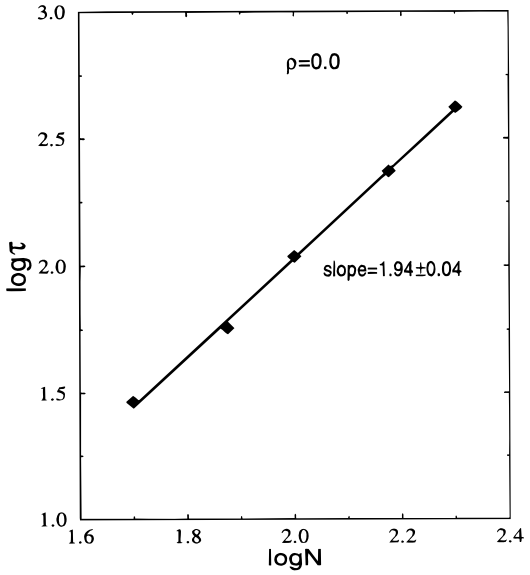

Figure 7. Normal mode relaxation times τ vs the size of the chains for systems at infinite dilution.

frequencies at higher densities, indicating an increase of the normal mode relaxation time.

The spectrum shapes are identical to the Rouse spectrum for low densities. For higher densities they broaden at the high-frequency side of the curves. For $N = 50$ the broadening is not considerable, even for densities larger than the estimated crossover density. For longer chains of $N = 150$, however, the spectrum shape changes considerably. These trends are illustrated in Figure 9, where the half-width Δ is plotted for systems with chains of size $N = 50$ and 150 at different densities. Δ is calculated normalizing the dielectric loss and the frequency with E''_{max} and f_{max} respectively. Then the $\log(f/f_{max})$ is computed and the width of the curves is found at $E''/E''_{max} = 0.5$ in decades of frequency. The horizontal dashed line is the half-width of the Rouse spectrum. There is significant noise in the data, resulting from errors in the calculation of the correlation function and the dielectric spectrum. These errors also result in the shoulders of some curves at the high frequency end of the spectrum as discussed in ref 16. Nevertheless, there is clearly a definite trend of broadening of the spectra with increasing density. This broadening can be attributed to overlapping of the chains that renders the relaxation of the macromolecules more heterogeneous. To elucidate the deviation of the dynamic behavior of the simulated systems at high densities from the Rouse model, we consider the normal modes of motion of the chains

$$\mathbf{X}_p(t) = \sqrt{\frac{N}{2}}\sum_{i=1}^{N}(\mathbf{r}_i(t) - \mathbf{r}_1(t))\cos\left[\frac{p\pi}{N}(i - 0.5)\right], \quad p \geq 1 \tag{19}$$

These modes decouple the motion of the chains to independent coordinates that decay as

$$\phi_p(t) = \langle \mathbf{X}_p(t)\cdot\mathbf{X}_p(0)\rangle/\langle \mathbf{X}_p{}^2\rangle = \exp(-t/\tau_p) \tag{20}$$

according to the Rouse theory, with $\tau_p = \zeta N^2 b^2/(3\pi^2 k_B T p^2)$, as described previously.

We calculate the first five modes using the simulation coordinates and plot the autocorrelation functions for chains with $N = 50$ and $N = 150$ beads at $\rho = 0.4$ vs a scaled time $t(\pi p)^2$ in Figure 10. The mode autocorrelation functions for $N = 50$ decay as single exponentials according to the theory. However, there is some slight curvature for $N = 150$, which implies a broader distribution of relaxation times than predicted by theory. In addition, although it seems that the scaled modes for chains with $N = 50$ roughly collapse onto a single curve, as the theory suggests, for chains with $N = 150$, the scaling of the mode relaxation times deviates significantly from the Rouse mode prediction. We have calculated the normal modes for all the simulated systems and we found that this deviation, whereas insignificant for short chains and highly diluted systems, becomes progressively pronounced for systems with longer chains at increased concentrations. This deviation results in the considerable broadening of the dielectric loss spectra for chains with $N = 150$ at the higher densities observed in Figure 8b. Freire and Adachi[39] observed similar behavior comparing the results of dynamic Monte Carlo simulations of polymers in good solvents by Rodriguez

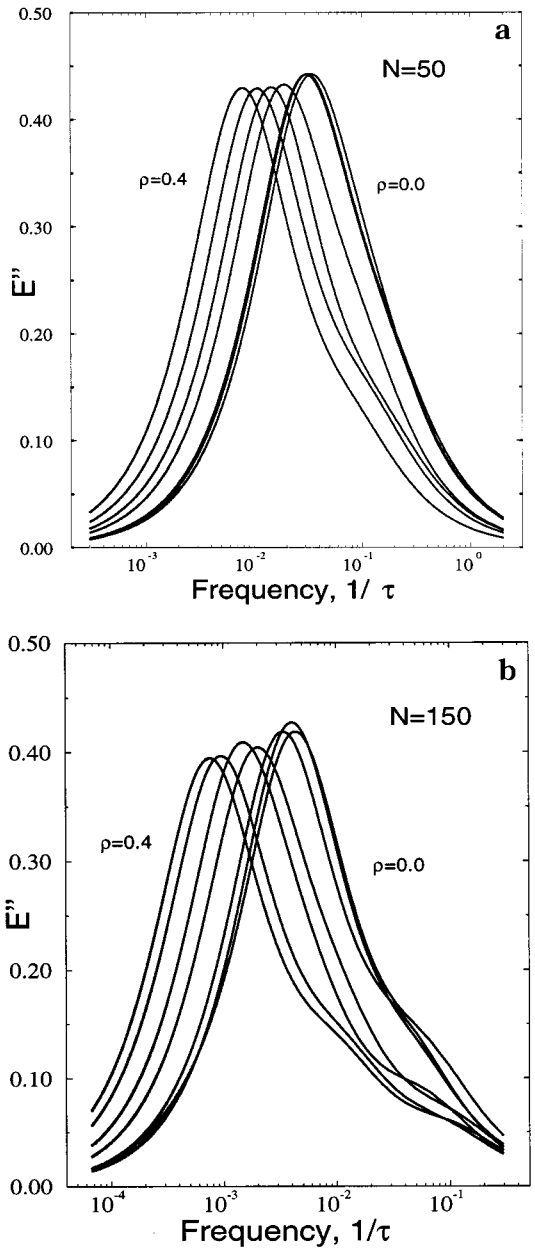

Figure 8. Dielectric loss spectra as a function of frequency for $N = 50$ (a) and $N = 150$ (b) at different densities ρ.

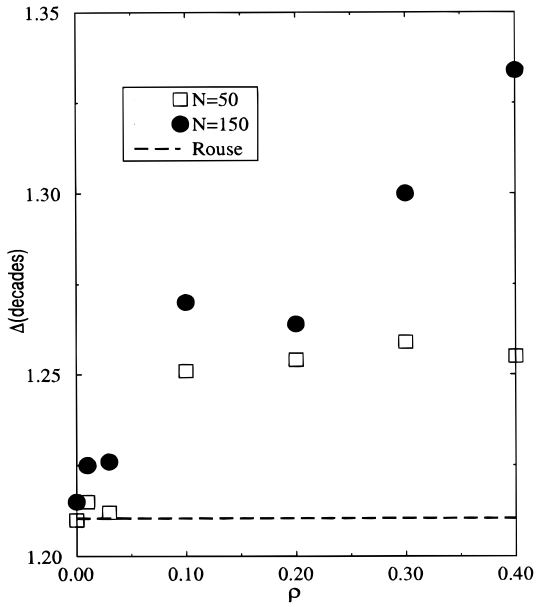

Figure 9. Half width Δ in decades of frequency for systems with $N = 50$ and 150 beads at different densitites ρ. The horizontal line is the half width of the Rouse spectrum.

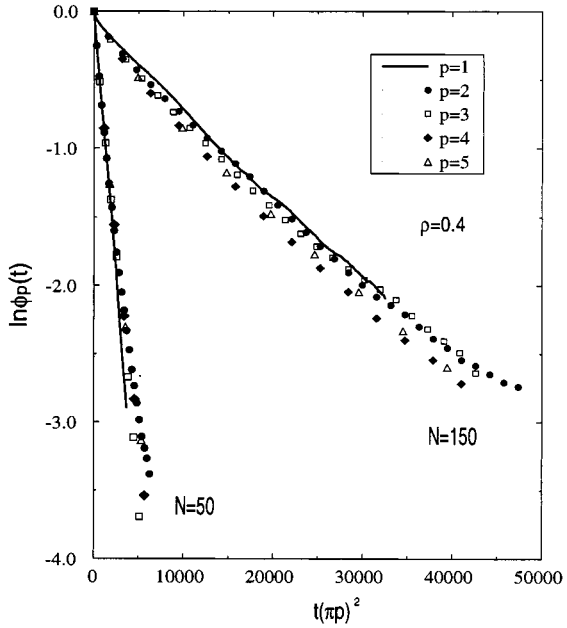

Figure 10. Normal mode autocorrelation functions for chains with $N = 50$ and $N = 150$ at $\rho = 0.4$ vs a reduced time $t(\pi p)^2$.

et al.[31] and dielectric spectroscopy experiments of PI in heptane, a good solvent, by Urakawa et al.[40]

To determine whether the broadening of the spectrum is exclusively a result of chain overlap we need to examine possible entanglement effects, since it has been suggested that entanglements affect the relaxation spectrum.[13] We calculate the mean squared displacement $g_1(t)$ for the five inner beads of the simulated systems.

$$g_1(t) = {}^1/_5 \sum_{i=N/2-2}^{N/2+2} \langle (\mathbf{r}_i(t) - \mathbf{r}_i(0))^2 \rangle \qquad (21)$$

Kremer and Grest suggested the use of only these five beads, so that the long chain behavior is revealed.[23] For nonentangled RW chains, three qualitatively different

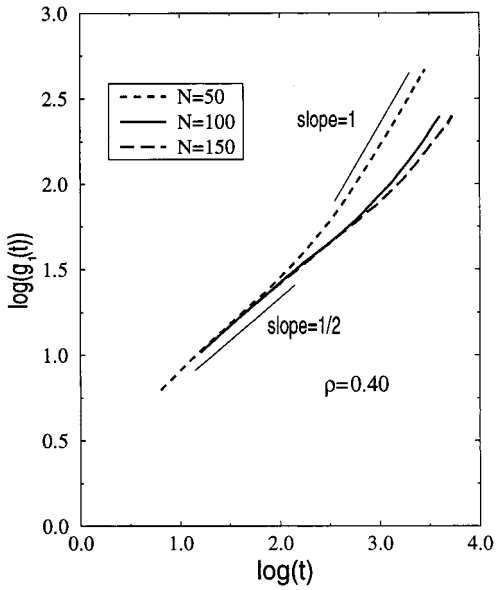

Figure 11. Double logarithmic plot of the mean squared displacement $g_1(t)$ as a function of time for chains of size N at $\rho = 0.4$.

regimes of chain motion can be distinguished[20,23] by different dependences of $g_1(t)$ on time

$$g_1(t) \propto \begin{cases} t, & t < \tau_C \\ t^{1/2}, & \tau_C < t < \tau_R \\ t, & t > \tau_R \end{cases} \qquad (22)$$

where τ_C is a characteristic relaxation time of local properties, such as chemical bonds, and τ_R is a characteristic relaxation time of polymer dimensions, such as the end-to-end distance. For entangled chains, the reptation theory[2] predicts five different regimes in the dynamic behavior of macromolecules

$$g_1(t) \propto \begin{cases} t, & t < \tau_C \\ t^{1/2}, & \tau_C < t < \tau_e \\ t^{1/4}, & \tau_e < t < \tau_R \\ t^{1/2}, & \tau_R < t < \tau_d \\ t, & t > \tau_d \end{cases} \qquad (23)$$

where τ_e is the entanglement time and τ_d is the disentanglement time.[2,3]

In Figure 11 $g_1(t)$ is plotted for systems of size N at $\rho = 0.4$. It is obvious that even for the system with $N = 150$ at $\rho = 0.4$ there are no entanglement effects. Therefore, the broadening of the dielectric loss spectra can be attributed solely to overlapping of the chains.

The normal mode relaxation times τ, calculated as the inverse of the maximum dielectric loss frequency, are given in Table 2. The relaxation times follow an exponential dependence with the density

$$\tau = \tau_o \exp(A\rho) \qquad (24)$$

where A is a constant ($A = 4.59$, 4.06, and 4.46 for $N = 50$, 100, and 150 respectively). This relation is clearly illustrated in Figure 12. This behavior can be explained in terms of the topological constraints, due to the uncrossability of the chains, that retard the rotational relaxation of macromolecules at increased densities. The exponential concentration dependence of the normal

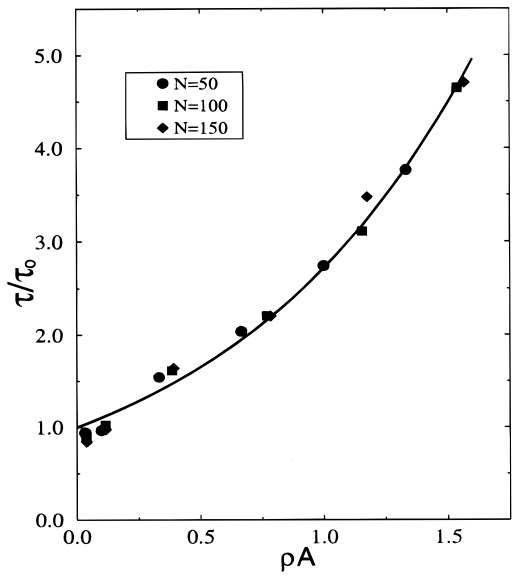

Figure 12. Reduced normal mode relaxation times τ/τ_o as a function of the reduced concentration ρA.

mode relaxation time was observed by Adachi and Kotaka for PI in dilute solutions of dioxane.[19] Phillies[41] deduced the simple exponential dependence for dilute solutions at the Θ point, using the hydrodynamic scaling model.[42] In a concentrated polymer solution, the hydrodynamic interactions are screened out. As a result the simulation relaxation times should coincide with the experimental ones. However, not many of the systems studied here are well into the concentrated regime. Consequently, we were unable to map our model dynamic parameter τ to real PI properties, as was achieved for the good solvent model.[16]

IV. Conclusions

Using equilibrium and nonequilibrium molecular dynamics, the concentration and chain size dependences of the dielectric strength, equilibrium conformations and dielectric loss spectra were studied for dilute and semidilute polymer solutions of a Θ solvent. The relation between the dielectric strength and the equilibrium end-to-end distance was established. Equilibrium conformations compared well with dielectric spectroscopy results and a mapping of the model static parameters to properties of *cis*-polyisoprene was proposed. The normal mode relaxation times at infinite dilution were found to conform with the scaling of the Rouse model. The broadening of the spectra of systems in the semidilute regime was attributed to overlapping of the chains, ruling out possible entanglement effects. Intermolecular chain interactions alter the modes of the chains motion, leading to deviations from the theoretical Rouse modes in both the form of the mode autocorrelation functions and the mode relaxation times scaling. Finally, the relaxation times were found to have an exponential dependence on density at the dilute and semidilute regimes in accordance with experimental observations.

Acknowledgment. We acknowledge financial support from the National Science Foundation (Grant CTS-9618777), the Army Research Office (Grant DAAG55-98-1-0091) and a generous allocation of computer time from the Boston Supercomputing Center. E.J.M. wishes to thank the National Science Foundation CAREER program (CTS-9701470). Y.N.K. wishes to thank the Fulbright Program for partial financial support.

References and Notes

(1) Flory, P. J. *Principles of Polymer Chemistry*; Cornell University: Ithaca, NY, 1953.
(2) Doi, M.; Edwards, S. F. *The Theory of Polymer Dynamics*; Clarendon Press: Oxford, England, 1986.
(3) De Gennes, P. G. *Scaling Concepts in Polymer Physics*; Cornell University: Ithaca, NY, 1979.
(4) Bird, R. B.; Curtiss, C. F.; Armstrong, R. C.; Hassager, O. *Dynamics of Polymeric Liquids*; John Wiley: New York, 1987; Vol. 2.
(5) Ferry, J. D. *Viscoelastic Properties of Polymers*; John Wiley: New York, 1980.
(6) Bicerano, J. *Prediction of Polymer Properties*; Marcel Dekker: New York, 1993.
(7) Van Krevelen, D. W. *Properties of Polymers*; Elsevier: Amsterdam, 1976.
(8) Rouse, P. E. *J. Chem. Phys.* **1953**, *21*, 1272.
(9) Zimm, B. H. *J. Chem. Phys.* **1956**, *24*, 269.
(10) Runt, J. P., Fitzgerald, J. J., (Eds.) *Dielectric Spectroscopy of Polymeric Materials*; American Chemical Society: Washington, DC, 1997.
(11) McCrum, N. G.; Read, B. E.; Williams, G. *Anelastic and Dielectric Effects in Polymeric Solids*; Dover: New York, 1991.
(12) Riande, E.; Saiz, S. *Dipole Moments and Birefrigence of Polymers*; Prentice Hall: Englewood Cliffs, NJ, 1992.
(13) Adachi, K.; Kotaka, T. *Prog. Polym. Sci.* **1993**, *18*, 585.
(14) Hedvig, P. *Dielectric Spectroscopy of Polymers*; Adam Hilger: Bristol, England, 1977.
(15) Stockmayer, W. H. *Pure Appl. Chem.* **1967**, *15*, 539.
(16) Kaznessis, Y. N.; Hill, D. A.; Maginn, E. J. *J. Chem. Phys.* **1998**, *109*, 5078.
(17) Van Kampen, N. G. *Stochastic Processes in Physics and Chemistry*; North-Holland: Amsterdam, 1981.
(18) Adachi, K.; Kotaka, T. *Macromolecules* **1987**, *20*, 2018.
(19) Adachi, K.; Kotaka, T. *Macromolecules* **1988**, *21*, 157.
(20) Binder, K., Ed. *Monte Carlo and Molecular Dynamics Simulations in Polymer Science*; Oxford University Press: New York, 1995.
(21) Roe, R. J., Ed. *Computer Simulations of Polymers*; Prentice Hall: Englewood Cliffs, NJ, 1991.
(22) Bicerano, J., Ed. *Computational Modeling of Polymers*; M. Dekker: New York, 1992.
(23) Kremer, K.; Grest, G. S. *J. Chem. Phys.* **1989**, *92*, 5057.
(24) Grest, G. S.; Kremer, K. *Phys. Rev. A* **1986**, *33*, 3628.
(25) Ermak, D. L.; McCammon, J. A. *J. Chem. Phys.* **1978**, *69*, 1352.
(26) Fixman, M. *J. Chem. Phys.* **1983**, *78*, 1594.
(27) Fixman, M. *J. Chem. Phys.* **1986**, *84*, 4085.
(28) Rey, A.; Freire, J. J.; De la Torre, J. D. *J. Chem. Phys.* **1989**, *90*, 2035.
(29) Rey, A.; Freire, J. J.; De la Torre, J. D. *Macromolecules* **1991**, *24*, 4666.
(30) Rey, A.; Freire, J. J.; De la Torre, J. D. *Polymer* **1990**, *33*, 3477.
(31) Rodriguez, A. L.; Freire, J. J. *Macromolecules* **1991**, *24*, 3578.
(32) Freire, J. J.; Rey, A.; Bishop M.; Clarke, J. H. R. *Macromolecules* **1991**, *24*, 6494.
(33) Rodriguez, A. L.; Rey A.; Freire, J. J. *Macromolecules* **1992**, *25*, 3266.
(34) Milchev, A.; Paul W.; Binder, L. *J. Chem. Phys.* **1993**, *99*, 4786.
(35) Grest, G. S.; Murat, M. *Macromolecules* **1993**, *26*, 3108.
(36) Kaznessis, Y. N.; Hill, D. A.; Maginn, E. J. *Macromolecules* **1998**, *31*, 3116.
(37) Olaj, O. F.; Pelinka, K. H. *Makromol. Chem.* **1976**, *177*, 3447.
(38) Olaj, O. F.; Petrik, T.; Zifferer, G. *J. Chem. Phys.* **1997**, *107*, 10214.
(39) Freire, J. J.; Adachi, K. *Macromolecules* **1995**, *28*, 4747.
(40) Urakawa, O.; Adachi, K.; Kotaka, T. *Macromolecules* **1993**, *26*, 2042.
(41) Phillies, G. D. J. *J. Phys. Chem. B* **1997**, *101*, 4226.
(42) Phillies, G. D. J. *Macromolecules* **1998**, *31*, 2317, and references therein.

MA981320U